Check for updates

Initiated Chemical Vapor Deposition Kinetics of Poly(4-aminostyrene)

Alexandra Khlyustova and Rong Yang*

Robert Frederick Smith School of Chemical and Biomolecular Engineering, Cornell University, Ithaca, NY, United States

Initiated Chemical Vapor Deposition (iCVD) is a free-radical polymerization technique used to synthesize functional polymer thin films. In the context of drug delivery, the conformality of iCVD coatings and the variety of functional chemical moieties make them excellent materials for encapsulating pharmaceutics. Poly(4-aminostyrene) (PAS) belongs to a class of functionalizable materials, whose primary amine allows decoration of the delivery vehicles with biomolecules that enable targeted delivery or biocompatibility. Understanding kinetics of PAS polymerization in iCVD is crucial for such deployments because drug release kinetics in thin-film encapsulation have been shown to be determined by the film thickness. Nevertheless, the effects of deposition conditions on PAS growth kinetics have not been studied systematically. To bridge that knowledge gap, we report the kinetics of iCVD polymerization as a function of fractional saturation pressure of the monomer (i.e., P_m/P_{sat}) in a dual-regime fashion, with quadratic dependence under low P_m/P_{sat} and linear dependence under high P_m/P_{sat}. We uncovered the critical P_m/P_{sat} value of 0.2, around which the transition also occurs for many other iCVD monomers. Because existing theoretical models for the iCVD process cannot fully explain the dual-regime polymerization kinetics, we drew inspiration from solution-phase polymerization and proposed updated termination mechanisms that account for the transition between two regimes. The reported model builds upon existing iCVD theories and allows the synthesis of PAS thin films with precisely controlled growth rates, which has the potential to accelerate the deployment of iCVD PAS as a novel biomaterial in controlled and targeted drug delivery with designed pharmacokinetics.

Keywords: polymer, kinetics, deposition rate, initiated Chemical Vapor Deposition, activation energy, thin films, 4-aminostyrene, controlled drug release

INTRODUCTION

Polymers have been widely used as the encapsulation material to enable controlled release of pharmaceutics due to their desirable properties such as biocompatibility, mechanical flexibility, rich functional moieties, and cost-effective manufacturing (Khlyustova et al., 2020). Although polymer particles and hydrogels have remained the most prevalent drug delivery vehicles (Perrotta et al., 2018), polymer thin films have emerged in recent years as an alternative that

could enable programmable drug release kinetics through precise film thickness control (Ghasemi-Mobarakeh et al., 2019; Sayin et al., 2019; Decandia et al., 2020).

While existing polymer thin films in drug delivery have commonly relied on solution synthesis and processing (Ré, 2006), solvent-free techniques such as initiated Chemical Vapor Deposition (iCVD) offer distinct advantages over the conventional approaches, including elimination of solvents and improved control over film thickness. Dichloromethane, ethyl acetate, and silicone oil have been used in the spray drying of poly(D,L-lactic acid) to obtain a thin film that encapsulated bovine serum albumin for a parenteral delivery system (Gander et al., 1996). To avoid acutely toxic solvents such as dichloromethane, water and ethanol have been used in encapsulation of albendazole (used for treatment of echinococcosis). Nevertheless, this approach is limited to water-soluble polymers such as polyvinyl alcohol, polyvinyl pyrrolidone, and hydroxypropyl methylcellulose (Alanazi et al., 2007), which commonly lead to high dissolution rates and thereby high and hard-to-control release rates *in vivo* (Ni et al., 2017). In addition to solvent toxicity, the choice of appropriate solvents is further constraint by potential solvent-mediated degradation of active therapeutic ingredients (Christian et al., 2016; Qiu et al., 2020). Furthermore, the solution methods allow limited control over thickness of the encapsulating polymer films. To address the limitations of the solution-based techniques, the solvent-free polymerization technique, iCVD, has been employed to synthesize encapsulation coatings in drug delivery (Coclite et al., 2013; Sayin et al., 2019). To date, the versatile iCVD technique has been used to encapsulate highly soluble antibiotic gentamicin (Decandia et al., 2020), to enable the controlled release of phenytoin and indomethacin (Christian et al., 2018; Werzer et al., 2019), and to fabricate wound dressing that releases clotrimazole (Ghasemi-Mobarakeh et al., 2019). Copolymers of methacrylic acid (MAA) has enabled enteric drug delivery via its pH-dependent swelling, which increased the mesh size in alkaline environments (Lau and Gleason, 2007). Using a similar iCVD polymer, camptothecin was released at a slow rate at pH of 1.8 and a controllable high rate at pH of 7.4 (McInnes et al., 2012). In the aforementioned study of gentamicin encapsulation, copolymers of MAA retained the antibacterial activity (Decandia et al., 2020).

Initiated Chemical Vapor Deposition enables all-dry free radical polymerization. During iCVD, the substrates to be coated (e.g., films of pharmaceutics) are placed on a temperature-controlled stage and thus kept under room-temperature and solvent-free conditions throughout the one-step polymerization and film formation, retaining the full activities of labile pharmaceutics. The iCVD precursors (i.e., initiator and monomers) enter the reactor chamber under medium vacuum, where the monomers adsorb onto the substrate surface (e.g., a drug film) and the initiator breaks down into radicals (Lau and Gleason, 2006b; Zhao et al., 2017), which initiate polymerization upon surface impingement (Tenhaeff and Gleason, 2008; Decandia et al., 2020). Furthermore, iCVD is often implemented with an *in situ* interferometry that allows nanometer-scale control of the thickness of the film grown on a reflective substrate (e.g., a silicon wafer). Despite that film thickness control on

reflective substrates, polymer growth kinetics on non-reflective substrates (such as porous substrates or drug films) could differ considerably from that on a silicon wafer (Cheng et al., 2020). As a result, deep understanding of the iCVD polymerization kinetics is required to enable precise control of the thickness of encapsulation layers and of drug release kinetics.

Here, we demonstrated improved understanding of the iCVD kinetics using the monomer 4-aminostyrene (AS). AS was chosen because its primary amine group enables further functionalization by biomolecules including antibodies, enzymes and genetic materials (e.g., RNAs and DNAs). For example, amide bond between a primary amine and a carboxylic acid has been commonly used in biocoupling reactions such as peptides (Li et al., 2020) or antibody immobilization (Maraldo and Mutharasan, 2007). Another example is a reaction between primary amine and aldehyde via nucleophilic addition, which enables functionalization by chitosan and other monosaccharides (Butler et al., 2003). Furthermore, poly(4-aminostyrene) (PAS) is known to be pH-responsive, hydrophobic in neutral pH and soluble in acidic pH (Wang et al., 2014), enabling accelerated drug release under acidic environments such as tumor tissues with pH as low as 5.7 (Cao et al., 2019).

Despite the plethora of potential applications in drug delivery and biomaterials, the growth kinetics of iCVD PAS remain elusive. Details about the iCVD polymerization of AS, such as the rate law with respect to monomer concentration and stage temperature, have not been reported, potentially limiting the ability to achieve controlled drug release kinetics. To address that challenge, this report provides detailed understanding of the effects of the fractional saturation pressure of monomer (P_m/P_{sat}) and stage temperature on the rate of PAS film growth. Distinct from the previously observed iCVD kinetics (Lau and Gleason, 2006a,b), where rate of polymerization depends on P_m/P_{sat} in a quadratic fashion, we captured two regimes of the rate dependence. In a narrow range of low P_m/P_{sat} (specifically, $P_m/P_{sat} < 0.2$), the rate of deposition was proportional to $(P_m/P_{sat})^2$, which has been observed in solution free-radical polymerization when primary radical termination dominates (Bamford et al., 1959) (taking the approximation that P_m/P_{sat} is comparable to [M], bulk monomer concentration). At high P_m/P_{sat}, rate of deposition depends linearly on (P_m/P_{sat}), consistent with the solution free-radical polymerization when disproportionation or combination is the dominating termination mechanism. That has also been corroborated by several previous reports on iCVD polymerization (Tenhaeff and Gleason, 2008; Ozaydin-Ince and Gleason, 2009), but the systematic characterization of the full continuum from quadratic to linear transition has not been achieved. In addition, we uncovered the critical P_m/P_{sat} value of 0.2, around which the quadratic-to-linear transition occurs for many iCVD monomers (Gupta and Gleason, 2006; Ozaydin-Ince and Gleason, 2009). The reported kinetics study enables the accurate prediction and detailed tuning of the growth kinetics of a highly functionalizable polymer PAS synthesized using a state-of-the-art all-dry polymerization technique, iCVD. The capability to predict and control the growth of PAS thin films has the potential to enable novel designs of targeted and smart

drug delivery vehicles with well understood release kinetics and thereby pharmacokinetics, accelerating materials design, and deployment in healthcare.

MATERIALS AND METHODS

Chemicals and Materials

4-aminostyrene (97%, Sigma-Aldrich), tert-butyl peroxide (TBPO, 98%, Sigma-Aldrich) were both used as received without further purification.

The iCVD Setup

All polymerization reactions were done in a custom-built iCVD reactor chamber (335 mm diameter, 51 mm height, schematic shown in **Figure 1**), which was evacuated by an E2M40 rotary vane vacuum pump (Edwards Vacuum, United Kingdom). During deposition, AS was heated to 75–85°C and total reactor pressure was kept at 0.350 Torr, well within the common pressure range used in iCVD processes (i.e., 0.1–1 Torr) (Tenhaeff and Gleason, 2008) while being on the low end of that range. The pressure was selected in this work in consideration of potential applications for the polymer thin films of PAS in drug delivery, where conformal coatings (which are commonly associated with lower P_m/P_{sat} and thus lower total pressure) are most desirable. Furthermore, the pressure chosen was shown to avoid condensation on the reactor lid and stage, which tend to happen at higher pressure values even with the low monomer flow rate used in this work. The filament temperature was kept at 250–260°C for all experiments, selected to be consistent with previous reports on PAS (Xu and Gleason, 2010). P_m/P_{sat} was changed by varying stage temperature or monomer flow rate

(see **Supplementary Material section** "Process Conditions for Initiated Chemical Vapor Depositions of Poly(4-aminostyrene)" for details). The initiator flow rate was kept constant at 0.50 ± 0.02 sccm. Due to the non-volatile nature of AS, inert gas was not included such that measurable deposition rates can be obtained. The variation in total flow rate caused by the absence of inert gas is ≤ 0.25 sccm among all depositions, which is small enough to not change the deposition kinetics significantly, as evidenced by the excellent fit between experimental data and theoretical predictions that were made based on this assumption (see **Figure 3**).
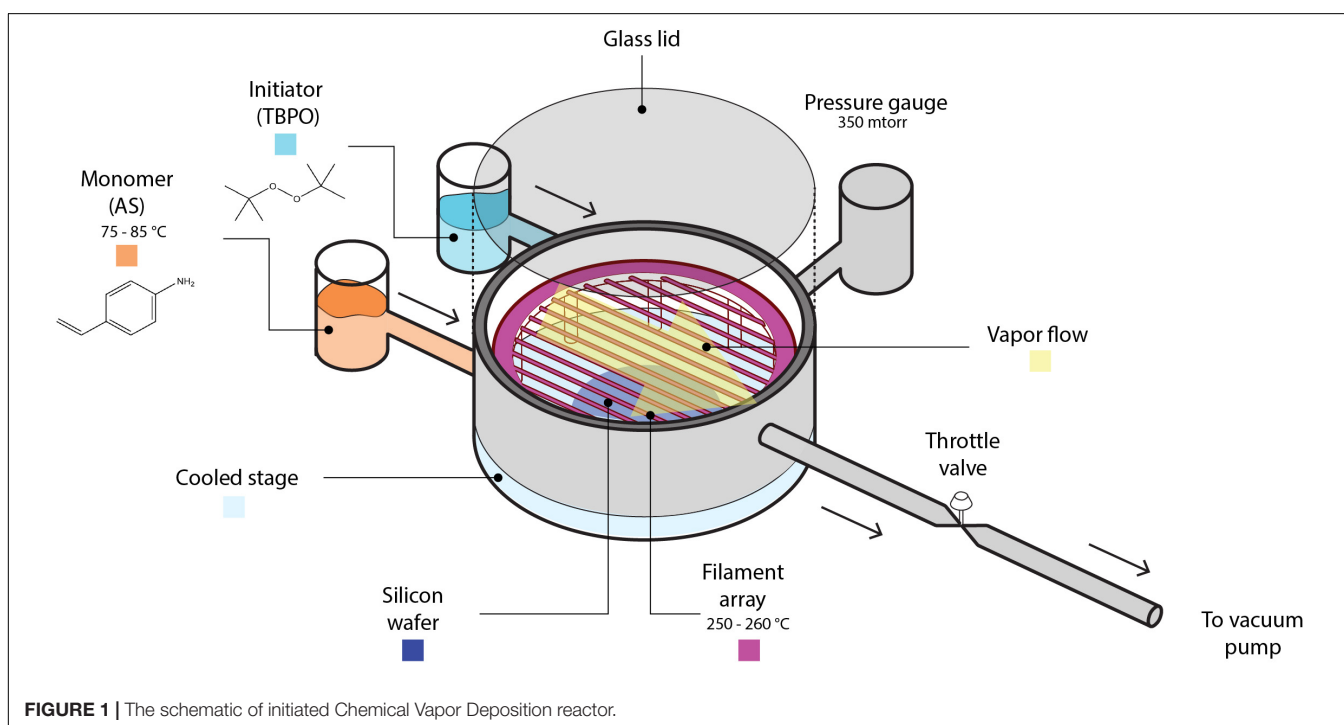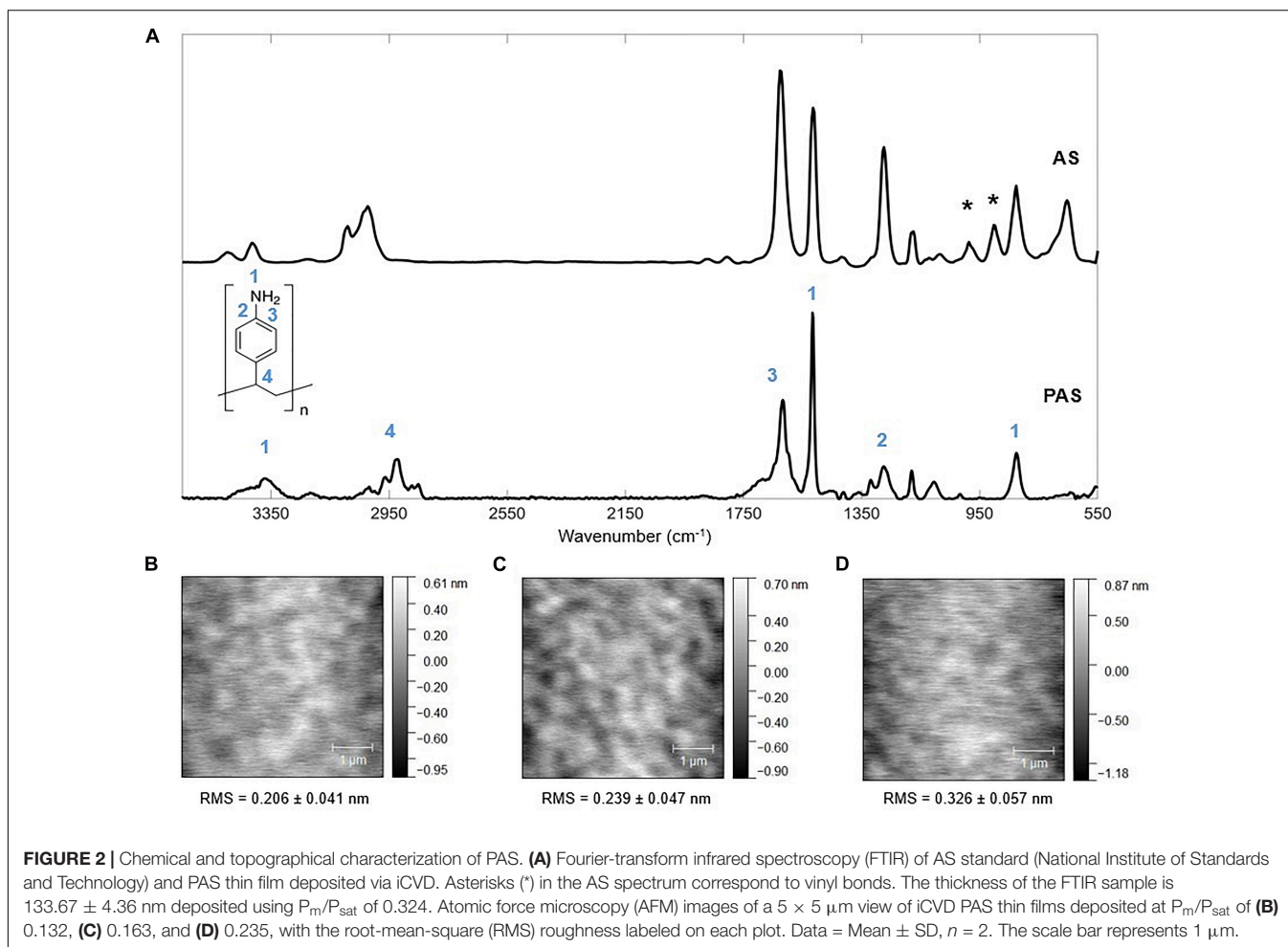
Chemical Characterization

Fourier-transform infrared spectroscopy (FTIR) was used to determine film composition. Thickness of the thin films was measured by ellipsometry. See **Supplementary Material section** "Chemical and Topographical Characterization" for details.

RESULTS AND DISCUSSION

Chemical Composition and Topography of the iCVD PAS Thin Films

To confirm the obtainment of the PAS molecular structure via iCVD polymerization, FTIR was applied to iCVD-deposited PAS with the thickness of ∼ 200 nm. The spectra of iCVD PAS and an AS standard (from National Institute of Standards and Technology) are shown in **Figure 2A** along with the chemical structure of PAS. FTIR spectra were collected for samples deposited under each set of conditions listed in **Supplementary Table 1**, and they were identical to **Figure 2A**.

FIGURE 1 | The schematic of initiated Chemical Vapor Deposition reactor.

FIGURE 2 | Chemical and topographical characterization of PAS. **(A)** Fourier-transform infrared spectroscopy (FTIR) of AS standard (National Institute of Standards and Technology) and PAS thin film deposited via iCVD. Asterisks (*) in the AS spectrum correspond to vinyl bonds. The thickness of the FTIR sample is 133.67 ± 4.36 nm deposited using P_m/P_{sat} of 0.324. Atomic force microscopy (AFM) images of a $5 \times 5\,\mu m$ view of iCVD PAS thin films deposited at P_m/P_{sat} of **(B)** 0.132, **(C)** 0.163, and **(D)** 0.235, with the root-mean-square (RMS) roughness labeled on each plot. Data = Mean $\pm$ SD, $n = 2$. The scale bar represents $1\,\mu m$.

Therefore, a representative spectrum, collected on samples deposited with the P_m/P_{sat} value of 0.324 is shown here. In the spectrum of PAS, the absence of peaks corresponding to =CH and =CH$_2$ bending (which occurred at around 900 cm^{-1} and labeled with asterisks for AS) proved that polymerization was complete. Furthermore, despite the observed difference in peak intensities between the AS monomer standard and iCVD PAS (e.g., the relative peak intensities of 1 and 3 in **Figure 2A**), the spectrum of iCVD PAS agreed well with the literature (Cha et al., 2016). Each peak that corresponds to a functional moiety in the PAS was labeled with a numerical index to match the labeling on the molecular structure in **Figure 2A**. For example, there were three peaks corresponding to the N-H bond, all labeled with "1." N-H stretching led to a few weak peaks located at $\sim$ 3400 cm^{-1}. At around 1516 cm^{-1} there was a medium peak due to N-H bending of the primary amine. The peak at 825 cm^{-1} corresponded to the N-H out-of-plane bending (i.e., N-H wagging). The peak located at 1271 cm^{-1} (labeled with "2") corresponded to the C-N stretching adjacent to the phenyl group. The peak at 1620 cm^{-1} (labeled with "3") was due to C=C stretching in the aromatic ring. The peak at around 3000 cm^{-1} (labeled with "4") corresponded to C-H stretching that was a result of the combined effect of the C-H next to the phenyl group and those in the polymer backbone.

Therefore, the FTIR spectrum supported that PAS was obtained successfully by using iCVD.

Atomic force microscopy (AFM) in **Figures 2B–D** captures PAS topography at different P_m/P_{sat}. The surface roughness of all films was <0.5 nm, confirming the ultra-smoothness of the iCVD polymer films. The surface roughness increased slightly from 0.206 ± 0.041 nm for P_m/P_{sat} of 0.132 to 0.326 ± 0.057 nm for P_m/P_{sat} of 0.235. That mild increase in surface roughness upon increasing P_m/P_{sat} can be explained by a minor increase in the sticking probability of free radicals, i.e., a higher likelihood of surface impingement upon collision of radicals on the monomer-adsorbed surface, hence, greater rate of localized initiation of polymerization, which ultimately led to slightly increased surface roughness. The same effect reduces conformality of thin films deposited over nano-structured substrates, as shown in **Supplementary Material section** "Conformality of PAS in 3D Structures."

Rate Laws for the iCVD of PAS

Similar to solution-based free radical polymerization, the kinetics iCVD have been shown to be controlled by the surface concentration of monomers, [M] (moles/m^3), which is proportional to the monomer fractional saturation pressure,

P_m/P_{sat}, i.e., the ratio of monomer partial pressure to its saturation pressure at the temperature of the stage (Lau and Gleason, 2006a,b). P_m/P_{sat} is proportional to the monomer surface concentration because the surface adsorption of monomers in iCVD has been shown to follow the Brunauer–Emmett–Teller (BET) isotherm (Lau and Gleason, 2006a,b). The BET theory describes the equilibrium of multilayer physisorption, where each surface site (i.e., the surface area occupied by a single molecule) is assumed to have the same adsorption energy and only molecules in adjacent layers are assumed to have interactions (Brunauer et al., 1938). Applying the BET theory to describe the monomer physisorption in iCVD yields (Lau and Gleason, 2006a,b):

$$[M] = \frac{\rho_M}{M} \times \frac{c \times \frac{P_m}{P_{sat}}}{\left(1 - \frac{P_m}{P_{sat}}\right) \times \left(1 - (1-c) \times \frac{P_m}{P_{sat}}\right)} \quad (1)$$

$$\lim_{\frac{P_m}{P_{sat}} \to 0} [M] \approx \frac{\rho_M}{M} \times c \times \frac{P_m}{P_{sat}} \quad (2)$$

where ρ_M is density of liquid monomer, which is 1017 kg/m^3 here (i.e., the density of AS) (Sharma et al., 2019); M is the molar mass of AS, i.e., 0.119 kg/mol; c is the BET constant, which represents the energy of monolayer adsorption (Ambroz et al., 2018). By assuming the enthalpy of desorption for the first layer (i.e., at the monomer-substrate interface) to be constant and greater than that of the second layer (i.e., the heat of vaporization), the BET constant can be calculated using the Arrhenius law for desorption (Duncan, 1949):

$$c = \exp\left[\frac{\Delta H_{des} - \Delta H_{vap}}{RT_{stage}}\right] \quad (3)$$

where T_{stage} is stage temperature in iCVD, R is a gas constant {i.e., 8.314 [J/ (mol K)]}, ΔH_{des} and ΔH_{vap} are enthalpy of desorption and heat of vaporization, respectively. The heat of vaporization of AS has been calculated from simulations to be 47.6 ± 3.0 kJ/mol (ChemSpider, 2020); whereas the reported enthalpy of desorption for styrene, which is 61 kJ/mol, was used to approximate ΔH_{des} for the monomer AS (Ranke and Weiss, 2000). As such, the BET constant, c, for AS was calculated to be 1.005.

Consistent with the existing theories of iCVD (Lau and Gleason, 2006a,b), here we assumed that the rate of deposition is independent of the initiator concentration. That assumption has been recently validated in experiments, where radicals were shown to be generated in such abundance that the chemisorption of radicals, i.e., the initiation step of the iCVD polymerization, was not the rate-limiting step under regular iCVD conditions (Şimşek and Karaman, 2020). As a result, the rate of iCVD polymerization can be expressed in terms of P_m/P_{sat}, as follows:

$$R_{poly}\,(\text{flat}) = k \times [M]^\alpha = k' \times \left[\frac{P_m}{P_{sat}}\right]^\alpha \quad (4)$$

where α is the order of reaction; $\alpha = 1$ for termination via disproportionation or combination, and $\alpha = 2$ for termination by primary radical termination, consistent with the reported rate

laws for solution-based free radical polymerization (Bamford et al., 1959). Previously, the rate law for iCVD kinetics has been expressed as either a quadratic dependence (Lau and Gleason, 2006b,a) or a linear dependence (Janakiraman et al., 2015); whereas here, we adopted this unifying expression to capture the full continuum from quadratic to linear transition as discussed below. The reaction rate coefficient, k, can be calculated using the Arrhenius relation (Laidler, 1984):

$$k = A \times \exp\left(-\frac{E_{a,\text{overall}}}{RT_{stage}}\right) \quad (5)$$

where A is the pre-exponential factor, depicting the collision frequency between reacting molecules; R, T_{stage}, and k are as described previously. The Eqs 4 and 5 combined offered an approach to correlate the rate of polymerization (experimentally measured via deposition rate, see **Supplementary Material section** "Calculation of Rate of Polymerization" for the detailed derivation for calculating rate of polymerization using deposition rate) with the monomer surface concentration (experimentally measured via P_m/P_{sat}), and thereby to regress for the rate constant (k) and order of reaction (α):
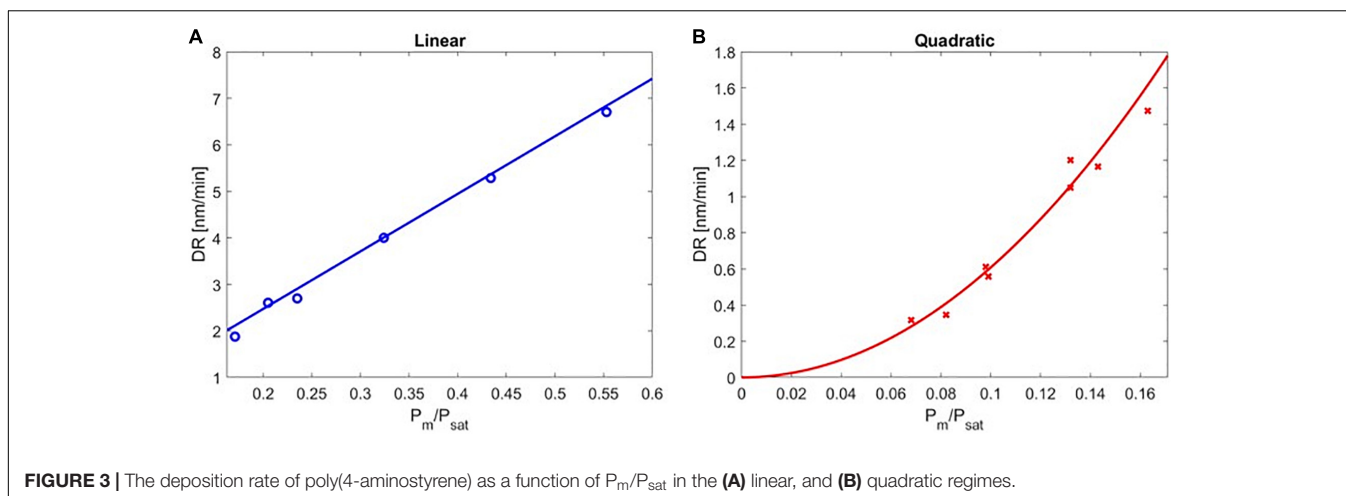
$$DR = k \times \frac{M \times h_{ml}}{\rho_p} \times \left(\frac{\rho_M}{M} \times c \times \frac{P_m}{P_{sat}}\right)^\alpha = k' \times \left[\frac{P_m}{P_{sat}}\right]^\alpha \quad (6)$$

where k' is an empirical rate constant, which took on the values of 11.517 and 68.08 in Eqs 7 and 8, respectively.

The Order of Reaction for the iCVD of PAS

The experimentally obtained deposition kinetics of PAS are depicted in **Figure 3**. The rate of deposition was plotted as a function of P_m/P_{sat} and divided into two regimes: the linear regime under high P_m/P_{sat} (**Figure 3A**) and the quadratic regime under low P_m/P_{sat} (**Figure 3B**). The transition point between the linear and the quadratic regimes was determined using a statistical approach (see **Supplementary Material section** "Quantification of the Transition Point" for details).

DR of PAS increased linearly with P_m/P_{sat} from 0.171 to 0.553, indicating the rate of the polymerization had first-order dependence on the monomer surface concentration (the maximum value of P_m/P_{sat} that could be obtained without causing local condensation in the iCVD reactor was 0.553). It is important to note that DR of PAS was extremely slow (<7 nm/min), consistent with the previously reported rate of deposition (Gleason and Xu, 2013). This first-order kinetic dependence agreed with solution-based free-radical polymerization, where the polymerization rate is proportional to the concentration of monomer [M] when chain termination is dominated by disproportionation or combination. That linear dependence on [M] originated from the pseudo-steady state approximation (Hiemenz and Lodge, 2007), where the rate of monomer consumption is assumed to represent the rate of chain growth, and the rates of initiation and termination are assumed to be equal. In addition, the rate of initiation is assumed to be dominated by primary radical dissociation, which is monomer-independent, while initiation of polymer chain can be neglected due to its fast reaction rate (long chain approximation). In this

FIGURE 3 | The deposition rate of poly(4-aminostyrene) as a function of P_m/P_{sat} in the **(A)** linear, and **(B)** quadratic regimes.

linear regime, the data in **Figure 3A** can be regressed with a high coefficient of determination ($R^2 = 0.955$, with the maximum error in this region being ± 0.209 nm/min for P_m/P_{sat} of 0.171, corresponding to an 8% range) by the following equation:

$$\text{DR} = 11.517 \left(\frac{P_m}{P_{sat}} \right). \tag{7}$$

Consistent with previous iCVD studies, DR increased with greater P_m/P_{sat} values (Lau and Gleason, 2006a). The empirical rate constant for the linear regime, i.e., 11.517 nm/min, was comparable to the reported values for other iCVD polymerizations. For example, poly(vinylpyrrolidone), also a non-volatile monomer, had an empirical rate constant of approximately 5.26 nm/min in the linear regime (Janakiraman et al., 2015), while a more reactive monomer, cyclohexyl methacrylate, led to an empirical rate constant of $\sim$100 in the linear regime (Baxamusa and Gleason, 2008). Comparatively, AS belongs to a class of monomers with relatively slow deposition kinetics among the iCVD monomers reported to date.

DR of PAS followed a quadratic dependence on the P_m/P_{sat} in the range of 0.082 to 0.171. The resulting DR was even slower than that in the linear regime (<2 nm/min in the quadratic regime), which was expected due to the low concentration of surface monomers. This second-order kinetic dependence also agreed with solution-based free-radical polymerization, when chain termination is dominated by primary radical termination (Bamford et al., 1959). Under these conditions, the pseudo-steady state approximation applies and thus rate of initiation is equal to rate of primary radical termination. As a result, the concentration of growing chains is proportional to the concentration of monomers, leading to the quadratic dependence of polymerization rate on monomer concentration (Goodner and Bowman, 1999). In this quadratic regime, the data in **Figure 3B** can be regressed as follows ($R^2 = 0.994$, with the maximum error of ± 0.153 nm/min, occurred at P_m/P_{sat} of 0.163 ± 0.008).

$$\text{DR} = 69.08 \left(\frac{P_m}{P_{sat}} \right)^2 \tag{8}$$

The second-order dependence of DR for low P_m/P_{sat} values was also consistent with the previous studies, where the deposition of ethyl acrylate was found to vary with P_m/P_{sat} in a quadratic fashion when $P_m/P_{sat} < 0.04$ (Lau and Gleason, 2006a,b).

Note that the range of P_m/P_{sat} values shown in **Figure 3B** were obtained using a combination of two strategies, i.e., varying P_m and/or varying T_{stage} (due to the limited flow rate range one could achieve for a non-volatile monomer like AS). The separate datasets for each strategy (i.e., varying P_m/P_{sat} or substrate temperature) were included in **Supplementary Figure 2**. The error bar in **Supplementary Figure 2D** represents the results of four independent depositions performed under the same conditions, i.e., the highest P_m/P_{sat} (0.163 ± 0.008) in the quadratic regime with the DR of 1.473 ± 0.113 nm/min. Despite the difference in experimental conditions, the datasets followed an identical quadratic trend with a high coefficient of determination, further confirming the validity of the assumptions.

The Rate Constants for the iCVD of PAS

To provide reliable predictions for the iCVD rate of polymerization or DR in both regimes, Eq. 6 was used to regress for values of the rate constant, k, in both regimes. In this section, only datasets obtained under identical stage temperatures were used (see **Supplementary Table 1** samples PAS3 and PAS10–PAS14), with the consideration that the rate constant, k, is a function of temperature (Eq. 5). The iCVD reaction constant was calculated to be 0.064 ± 0.006 L/ (mol s) for quadratic regime and 0.111 s^{-1} for the linear regime. The difference in those constants can be attributed to different termination mechanisms in these regimes. The constant in quadratic regime is twofold smaller since primary radical termination proceeds faster as primary radicals scavenge the growing chain, thus stopping the polymerization reaction leading to slower growth rate.

In solution phase, this reaction rate constant, k, in quadratic regime represents the overall effects of the propagation constant (k_p) multiplied by chain initiation constant (k_i) over primary radical termination constant (k_{tp}), while in linear regime,

the reaction rate constant takes into account the propagation constant (k_p), initiator dissociation constant (k_d) and its efficiency (f), as well as termination constant for combination and disproportionation (k_t) (Odian, 2004). In addition, the propagation constant is a function of the type of initiator, solvent, and the reaction temperature, making a direct comparison to iCVD polymerization challenging, especially given that monomer surface adsorption instead of radical initiation is often the rate-limiting step in iCVD, unlike the case for solution polymerization.

The Activation Energy for the iCVD of PAS

The experimental activation energy was determined by measuring the DR under different stage temperatures (**Figure 4**), and by regressing for the overall activation energy, $E_{a,overall}$, using Eq. 5. **Figure 4** shows the Arrhenius plot for the DR as a function of $1/T_{stage}$ for the linear (**Figure 4A**) and the quadratic (**Figure 4B**) regimes. As reported in the literature (Lau and Gleason, 2006a), the DR of PAS decreased with increasing stage temperature in both regimes, indicating negative values for the activation energy, which is a result of the adsorption-limited deposition kinetics (monomer adsorption is exothermic). According to the Arrhenius correlation (Eq. 5), the slopes in **Figure 4** represented $-E_{a,overall}/R$, and the overall activation energy for the iCVD of PAS was thus determined to be -68.56 kJ/mol for the linear regime and -122.15 kJ/mol for the quadratic regime.

Those experimentally obtained values of the iCVD activation energy were validated by an estimate made using the following correlation (Lau and Gleason, 2006a):

$$E'_{a,\text{overall}} = E_{a,\text{prop}} - \alpha \Delta H_{\text{des}} \qquad (9)$$
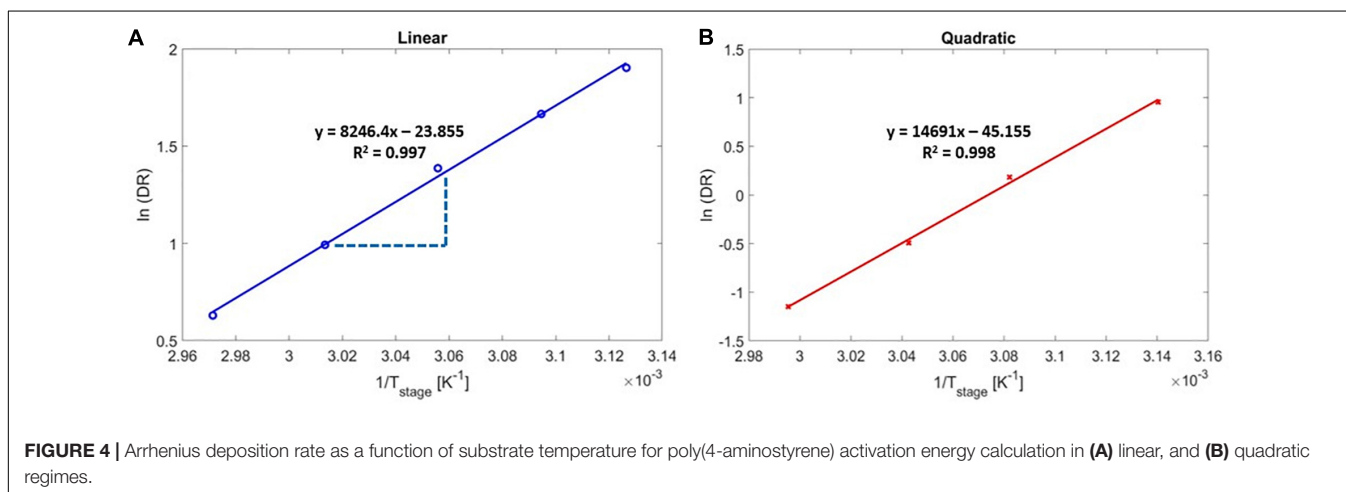
where $E'_{a,overall}$ is the estimated overall activation energy; $E_{a,prop}$ is the activation energy of the free radical polymerization of AS, which was assumed to be zero due to the adsorption-limited kinetics of iCVD (Lau and Gleason, 2006a); ΔH_{des} is the aforementioned heat of desorption; α is the order of reaction.

Using Eq. 9 with the order of reaction, $\alpha = 1$ (indicating the linear regime) yields a predicted value of ΔH_{des} of 61 kJ/mol. There is the small difference between the calculated activation energy, -61 kJ/mol, and experimentally measured activation energy, -68.56 kJ/mol, likely occurred due to collection of experimental data near the P_m/P_{sat} transition point of 0.163 ± 0.008.

In the quadratic regime (i.e., $\alpha = 2$), the experimental activation energy ($E_{a,overall} = -122.15$ kJ/mol) represented a strikingly close match to the estimated value of $E'_{a,overall} = 122$ kJ/mol, where $E'_{a,overall}$ was calculated using Eq. 9 and the previously reported ΔH_{des} value of 61 kJ/mol (Ranke and Weiss, 2000). That close match validated the accuracy of the experimental measurements and confirmed that the activation energy associated with free radical polymerization can be neglected.

This overall activation energy was also the smallest reported to date for iCVD due to the high enthalpy of desorption of the monomer AS. Despite that strong tendency to surface-adsorb, the DR of PAS was slow, which was likely a result of the small pre-exponential factor, A. Using Eq. 5, the pre-exponential factor, A, was determined to be 2.291×10^{10} s^{-1} for the linear regime (calculated using data in **Figure 4A**). This value fell on the low-end of surface-controlled reactions, which typically have a pre-exponential factor A $> 10^9$ s^{-1} (Genieva et al., 2010). The small pre-exponential factor and deposition kinetics of PAS can be explained by the partial transfer of electrons from the primary amine group to the vinyl group, reducing the probability of free radical initiation (Goikhman et al., 2011).

Interestingly, the critical P_m/P_{sat} value of 0.2, around which the transition from quadratic to linear regime occurred for the iCVD of PAS, could apply to other iCVD chemistries. For example, P_m/P_{sat} of 0.24 for poly(1H,1H,2H,2H-perfluorodecyl acrylate) (Gupta and Gleason, 2006) (PPFDA) and P_m/P_{sat} of 0.20 for poly(ethylene glycol diacrylate) (Ozaydin-Ince and Gleason, 2009). The generality was likely a result of the transition from a monolayer or less of adsorbed monomers, and thus primary radical termination dominates, to multilayer monomer

FIGURE 4 | Arrhenius deposition rate as a function of substrate temperature for poly(4-aminostyrene) activation energy calculation in **(A)** linear, and **(B)** quadratic regimes.

adsorption, which favors disproportionation or combination termination mechanisms.

CONCLUSION

The kinetics of the iCVD polymerization of AS were studied in great details. With low surface monomer concentration, the rate of polymerization/deposition varied with the surface monomer concentration in a quadratic fashion. Upon increasing the fractional saturation pressure of the monomer, i.e., P_m/P_{sat}, to values above 0.163 ± 0.008, the rate of polymerization/deposition depends linearly on the surface monomer concentration. The existence of these two regimes is consistent with the solution-based free radical polymerization, where the linear rate dependence applies to polymerization reactions terminated via disproportionation or combination and the quadratic rate dependence applies to those terminated by primary radical termination. Those distinct kinetic regimes were further corroborated by measurements of the overall iCVD activation energies in each regime, where the value of 68.56 kJ/mol was obtained for the linear regime and that of 122.15 kJ/mol for the quadratic regime. The latter represented a striking match with the theory-derived estimation (122 kJ/mol) made by using the enthalpy of adsorption for polystyrene. To enable facile estimation of the DR under varying deposition conditions, the iCVD rate constants in each regime were calculated using the experimental data reported here. The overall rate constant for the linear regime was $0.111~\text{s}^{-1}$ and that for the quadratic regime was 0.064 L/ (mol s). The constants were different due to dominance of different termination mechanism in each regime. However, it is still not clear how iCVD constants correlate with solution-phase constants since iCVD is assumed to be initiator-independent. Future studies are needed to figure out contribution of initiation, propagation, and termination constants in the expression of iCVD reaction constants. These rate constants could be used to estimate deposition rates using the corresponding formulation of the rate law for each regime. The two distinct termination mechanisms that led to the quadratic and linear kinetics likely had significant impact on the molecular weight and polydispersity of the iCVD PAS. Nevertheless, despite our best effort, PAS cannot be deposited in sufficient quantities for a molecular-weight analysis using conventional approaches like gel permeation chromatography (GPC). This challenge is also evident from the literature as such molecular weight data do not exist for iCVD-synthesized PAS, despite the long history and high utility of this polymer. Quantifying the molecular weight and polydispersity of iCVD polymers synthesized using monomers with low volatility or reactivity is a key issue that require novel approaches, which will be the focus of our future studies.

The unifying kinetic model and kinetic parameters reported here will enable the precise estimation of the polymer thin film growth kinetics based on conditions or the *a priori* selection of synthesis conditions that lead to the desirable rate of polymerization. The precise control of polymerization kinetics and facile selection of synthesis conditions thus could allow the accelerated design and deployment of PAS-based drug delivery vehicles with controlled and/or predictable pharmacokinetics.

DATA AVAILABILITY STATEMENT

The original contributions presented in the study are included in the article/**Supplementary Material**, further inquiries can be directed to the corresponding author.

AUTHOR CONTRIBUTIONS

AK conducted the iCVD depositions and all characterization experiments. AK and RY contributed to the experimental design, data analysis, and results interpretation, and drafted the manuscript and/or edited it critically for important intellectual content. Both authors contributed to the article and approved the submitted version.

FUNDING

SUPPLEMENTARY MATERIAL

The Supplementary Material for this article can be found online at: https://www.frontiersin.org/articles/10.3389/fbioe.2021.670541/full#supplementary-material

REFERENCES

Alanazi, F. K., El-Badry, M., Ahmed, M. O., and Alsarra, I. A. (2007). Improvement of albendazole dissolution by preparing microparticles using spray-drying technique. *Sci. Pharm.* 75, 63–79. doi: 10.3797/scipharm.2007.75.63

Ambroz, F., Macdonald, T. J., Martis, V., and Parkin, I. P. (2018). Evaluation of the BET Theory for the characterization of meso and microporous MOFs. *Small Methods* 2:1800173. doi: 10.1002/smtd.201800173

Bamford, C. H., Jenkins, A. D., and Johnston, R. (1959). Termination by primary radicals in vinyl polymerization. *Trans. Faraday Soc.* 55, 1451–1460. doi: 10.1039/tf9595501451

Baxamusa, S. H., and Gleason, K. K. (2008). Thin polymer films with high step coverage in microtrenches by initiated CVD. *Chem. Vap. Depos.* 14, 313–318. doi: 10.1002/cvde.200806713

Brunauer, S., Emmett, P. H., and Teller, E. (1938). Adsorption of gases in multimolecular layers. *J. Am. Chem. Soc.* 60, 309–319. doi: 10.1021/ja01269a023

Butler, M. F., Ng, Y. F., and Pudney, P. D. A. (2003). Mechanism and kinetics of the crosslinking reaction between biopolymers containing primary amine groups and genipin. *J. Polym. Sci. Part A Polym. Chem.* 41, 3941–3953. doi: 10.1002/pola.10960

Cao, Z., Li, W., Liu, R., Li, X., Li, H., Liu, L., et al. (2019). pH- and enzyme-triggered drug release as an important process in the design of anti-tumor drug delivery systems. *Biomed. Pharmacother.* 118:109340. doi: 10.1016/j.biopha.2019.109340

Cha, J., Jin, S., Shim, J. H., Park, C. S., Ryu, H. J., and Hong, S. H. (2016). Functionalization of carbon nanotubes for fabrication of CNT/epoxy nanocomposites. *Mater. Des.* 95, 1–8. doi: 10.1016/j.matdes.2016.01.077

ChemSpider (2020). *Royal Society of Chemistry.* ChemSpider. Available online at: http://www.chemspider.com/Chemical-Structure.66344.html (accessed February 2, 2020)

Cheng, Y., Khlyustova, A., Chen, P., and Yang, R. (2020). Kinetics of all-dry free radical polymerization under nanoconfinement. *Macromolecules* 53, 10699–10710. doi: 10.1021/acs.macromol.0c01534

Christian, P., Ehmann, H. M. A., Coclite, A. M., and Werzer, O. (2016). Polymer encapsulation of an amorphous pharmaceutical by initiated chemical vapor deposition for enhanced stability. *ACS Appl. Mater. Interfaces* 8, 21177–21184. doi: 10.1021/acsami.6b06015

Christian, P., Tumphart, S., Ehmann, H. M. A., Riegler, H., Coclite, A. M., and Werzer, O. (2018). Controlling indomethacin release through vapor-phase deposited hydrogel films by adjusting the cross-linker density. *Sci. Rep.* 8:7134. doi: 10.1038/s41598-018-24238-w

Coclite, A. M., Lund, P., Di Mundo, R., and Palumbo, F. (2013). Novel hybrid fluoro-carboxylated copolymers deposited by initiated chemical vapor deposition as protonic membranes. *Polymer (Guildf).* 54, 24–30. doi: 10.1016/j.polymer.2012.11.004

Decandia, G., Palumbo, F., Treglia, A., Armenise, V., Favia, P., Baruzzi, F., et al. (2020). Initiated chemical vapor deposition of crosslinked organic coatings for controlling gentamicin delivery. *Pharmaceutics* 12:213. doi: 10.3390/pharmaceutics12030213

Duncan, J. F. (1949). The determination of the surface area of a solid from an adsorption isotherm. *Trans. Faraday Soc.* 45, 879–891. doi: 10.1039/tf9494500879

Gander, B., Johansen, P., Nam-Trân, H., and Merkle, H. P. (1996). Thermodynamic approach to protein microencapsulation into poly(D,L-lactide) by spray drying. *Int. J. Pharm.* 129, 51–61. doi: 10.1016/0378-5173(95)04240-7

Genieva, S. D., Vlaev, L. T., and Atanassov, A. N. (2010). Study of the thermooxidative degradation kinetics of poly(tetrafluoroethene) using iso-conversional calculation procedure. *J. Therm. Anal. Calorim.* 99, 551–561. doi: 10.1007/s10973-009-0191-4

Ghasemi-Mobarakeh, L., Werzer, O., Keimel, R., Kolahreez, D., Hadley, P., and Coclite, A. M. (2019). Manipulating drug release from tridimensional porous substrates coated by initiated chemical vapor deposition. *J. Appl. Polym. Sci.* 136, 47858. doi: 10.1002/app.47858

Gleason, K. K., and Xu, J. (2013). *Hard, Impermeable, Flexible and Conformal Organic Coatings.* Available online at: https://patents.google.com/patent/US8552131B1/en (accessed 23 September, 2020).

Goikhman, M. Y., Subbotina, L. I., Martynenkov, A. A., Smirnov, M. A., Smyslov, R. Y., Popova, E. N., et al. (2011). Synthesis and optical properties of copolymers of 4-aminostyrene with the side styrylquinoline chromophore groups. *Russ. Chem. Bull.* 60, 295–303. doi: 10.1007/s11172-011-0048-4

Goodner, M. D., and Bowman, C. N. (1999). Modeling primary radical termination and its effects on autoacceleration in photopolymerization kinetics. *Macromolecules* 32, 6552–6559. doi: 10.1021/ma9901947

Gupta, M., and Gleason, K. K. (2006). Initiated chemical vapor deposition of poly(1H,1H,2H,2H-perfluorodecyl acrylate) thin films. *Langmuir* 22, 10047–10052. doi: 10.1021/la061904m

Hiemenz, P. C., and Lodge, T. P. (2007). *Polymer Chemistry.* Boca Raton, FL: CRC Press.

Janakiraman, S., Farrell, S. L., Hsieh, C. Y., Smolin, Y. Y., Soroush, M., and Lau, K. K. S. (2015). Kinetic analysis of the initiated chemical vapor deposition of poly(vinylpyrrolidone) and poly(4-vinylpyridine). *Thin Solid Films* 595, 244–250. doi: 10.1016/j.tsf.2015.04.083

Khlyustova, A., Cheng, Y., and Yang, R. (2020). Vapor-deposited functional polymer thin films in biological applications. *J. Mater. Chem. B.* 8, 6588–6609. doi: 10.1039/d0tb00681e

Laidler, K. J. (1984). The development of the arrhenius equation. *J. Chem. Educ.* 61:494. doi: 10.1021/ed061p494

Lau, K. K. S., and Gleason, K. K. (2006a). Initiated Chemical Vapor Deposition (iCVD) of poly(alkyl acrylates): a kinetic model. *Macromolecules* 39, 3695–3703. doi: 10.1021/ma0601621

Lau, K. K. S., and Gleason, K. K. (2006b). Initiated Chemical Vapor Deposition (iCVD) of poly(alkyl acrylates): an experimental study. *Macromolecules* 39, 3688–3694. doi: 10.1021/ma0601619

Lau, K. K. S., and Gleason, K. K. (2007). All-dry synthesis and coating of methacrylic acid copolymers for controlled release. *Macromol. Biosci.* 7, 429–434. doi: 10.1002/mabi.200700017

Li, Q., Zhang, Y., Wu, Z., Huang, J., Yue, N., Huang, L., et al. (2020). Tyrosine-EDC conjugation, an undesirable side effect of the EDC-catalyzed carboxyl labeling approach. *Anal. Chem.* 93, 697–703. doi: 10.1021/acs.analchem.0c03487

Maraldo, D., and Mutharasan, R. (2007). Optimization of antibody immobilization for sensing using piezoelectrically excited-millimeter-sized cantilever (PEMC) sensors. *Sensors Actuators B Chem.* 123, 474–479. doi: 10.1016/j.snb.2006.09.034

McInnes, S. J. P., Szili, E. J., Al-Bataineh, S. A., Xu, J., Alf, M. E., Gleason, K. K., et al. (2012). Combination of iCVD and porous silicon for the development of a controlled drug delivery system. *ACS Appl. Mater. Interfaces* 4, 3566–3574. doi: 10.1021/am300621k

Ni, R., Muenster, U., Zhao, J., Zhang, L., Becker-Pelster, E. M., Rosenbruch, M., et al. (2017). Exploring polyvinylpyrrolidone in the engineering of large porous PLGA microparticles via single emulsion method with tunable sustained release in the lung: In vitro and in vivo characterization. *J. Control. Release* 249, 11–22. doi: 10.1016/j.jconrel.2017.01.023

Odian, G. (2004). *Principles of Polymerization.* Hoboken, NJ: John Wiley & Sons, Inc., doi: 10.1002/047147875x

Ozaydin-Ince, G., and Gleason, K. K. (2009). Transition between kinetic and mass transfer regimes in the initiated chemical vapor deposition from ethylene glycol diacrylate. *J. Vac. Sci. Technol. A Vacuum Surfaces Film* 27, 1135–1143. doi: 10.1116/1.3168553

Perrotta, A., Werzer, O., and Coclite, A. M. (2018). Strategies for drug encapsulation and controlled delivery based on vapor-phase deposited thin films. *Adv. Eng. Mater.* 20:1700639. doi: 10.1002/adem.201700639

Qiu, Z., Hammer, B. A. G., and Müllen, K. (2020). Conjugated polymers–Problems and promises. *Prog. Polym. Sci.* 100:101179. doi: 10.1016/j.progpolymsci.2019.101179

Ranke, W., and Weiss, W. (2000). Adsorption and thermal decomposition of ethylbenzene and styrene on Pt(111) studied by UPS and XPS. *Surf. Sci.* 465, 317–330. doi: 10.1016/S0039-6028(00)00721-4

Ré, M. I. (2006). Formulating drug delivery systems by spray drying. *Dry. Technol.* 24, 433–446. doi: 10.1080/07373930600611877

Sayin, S., Ozdemir, E., Acar, E., and Ince, G. O. (2019). Multifunctional one-dimensional polymeric nanostructures for drug delivery and biosensor applications. *Nanotechnology* 30:412001. doi: 10.1088/1361-6528/ab2e2c

Sharma, J., Ahuja, S., and Arya, R. K. (2019). Experimental designing of polymer-polymer-solvent coatings: Poly(styrene)-poly(ethylene glycol)-chlorobenzene coating. *Prog. Org. Coatings* 128, 181–195. doi: 10.1016/j.porgcoat.2018.11.036

Şimşek, B., and Karaman, M. (2020). Initiated chemical vapor deposition of poly(hexafluorobutyl acrylate) thin films for superhydrophobic surface modification of nanostructured textile surfaces. *J. Coatings Technol. Res.* 17, 381–391. doi: 10.1007/s11998-019-00282-7

Tenhaeff, W. E., and Gleason, K. K. (2008). Initiated and oxidative chemical vapor deposition of polymeric thin films: ICVD and oCVD. *Adv. Funct. Mater.* 18, 979–992. doi: 10.1002/adfm.200701479

Wang, Z., Xia, J., Luo, S., Zhang, P., Xiao, Z., Liu, T., et al. (2014). Versatile surface micropatterning and functionalization enabled by microcontact printing of poly(4-aminostyrene). *Langmuir* 30, 13483–13490. doi: 10.1021/la503393j

Werzer, O., Tumphart, S., Keimel, R., Christian, P., and Coclite, A. M. (2019). Drug release from thin films encapsulated by a temperature-responsive hydrogel. *Soft Matter.* 15, 1853–1859. doi: 10.1039/C8SM02529K

Xu, J., and Gleason, K. K. (2010). Conformal, amine-functionalized thin films by initiated chemical vapor deposition (iCVD) for hydrolytically stable microfluidic devices. *Chem. Mater.* 22, 1732–1738. doi: 10.1021/cm903156a

Zhao, J., Wang, M., and Gleason, K. K. (2017). Stabilizing the wettability of Initiated Chemical Vapor Deposited (iCVD) polydivinylbenzene thin films by thermal annealing. *Adv. Mater. Interfaces* 4:1700270. doi: 10.1002/admi.201700270